DRUG DEVELOPMENT AND INDUSTRIAL PHARMACY, 15(5), 759-800 (1989)

USE OF A COMPACTION SIMULATOR SYSTEM IN TABLETTING RESEARCH

I. Introduction to and initial experiments with the system

Metin ÇELIK and Keith MARSHALL *
Smith Kline & French Laboratories, King of Prussia, PA 19406

ABSTRACT

The components and principal operating features of a compaction simulator system are described. Initial experiments with 8 model materials, using single-ended and double-ended compression waveforms are reported. Data obtained at two tablet machine speeds (30 and 150rpm) and at two compressional pressure levels (80 and 400MPa) demonstrate a correlation between total work or average power consumed during the process and the tensile strength of the tablets. Non-linearity of Heckel plots and limited compliance with the Walker equation are also shown.

INTRODUCTION

Instrumented single-station and multi-station tablet presses have been widely used to investigate the compactional behaviour of numerous powders in the field of pharmaceutical technology (1-5). Systematic investigations have been facilitated by the introduction of compaction simulators which are designed specifically to be capable of mimicking the exact cycle of any tabletting process in real time and to record all important parameters during the cycle.

* Correspondence

Rees et al. (6) developed a device which was used with a single-acting mechanical press (Instron) to simulate the double-acting compression cycle of a multi-station tablet machine. However, this device was not capable of simulating the compaction cycle of a rotary press in real time. Çelik and Travers (7) used a computer-aided compaction simulator (Mayes Universal Hydraulic Testing Press), consisting of a servo-controlled hydraulic actuator mounted in a frame, to mimic the action of a single-station press.

The first so-called "true" compaction simulator to mimic the compression and ejection cycle of any tablet press at its normal operating speed was developed by Hunter et al. (8). Although during the last decade several other compaction simulators have been built, the number of reports in the literature with such machines is still small (9-12).

As can be seen from Table 1, which compares the hardware on which compaction studies can be carried out, compaction simulators have certain advantages over instrumented single or multi-station presses or isolated punch and die assemblies. In addition to these advantages, compaction simulators have numerous potential applications in pharmaceutical research, development and production, such as studying basic compaction mechanisms, process variables, scale-up parameters, trouble-shooting problem batches, creating compaction data banks and 'fingerprinting' new actives and excipients.

The aim here is to describe the commissioning of a new compaction simulator system and to present data obtained from initial experiments with model powders.

The phenomena and mechanisms involved during the compaction of pharmaceutical powders have been the subject of numerous publications during the last four decades. The equipment, the parameters monitored and the techniques used to assess the compactional behaviour varied widely. Data obtained from measurements of the forces and the displacement of the

TABLE 1. Comparison of Equipment for Tabletting Studies

Feature	single station press	multi station press	punch and die set	simulator
mimic production conditions	no	yes	maybe	yes
mimic cycles of many presses	no	no	maybe	yes
require small amount of material	yes	no	yes	yes
easy to instrument	yes	no	yes	yes
equipment inexpensive	yes	no	maybe	no
easy to set up	yes	no	maybe	maybe
data base in literature	yes	yes	some	no
used for stress/strain studies	no	no	yes	yes

upper and lower punches (4,5,13,14), axial to radial load transmission (15), die wall friction (14), ejection force (3) and temperature changes (16) have all been used to evaluate the deformation characteristics of a variety of pharmaceutical powders.

Many techniques have been employed to attempt to characterize the compressional process, but comprehensive analysis of the observed changes in volume is difficult due to the complexity of the systems being compressed. One of the most widely used approaches has been to try and develop simple relationships between the changing volume (or porosity) of the tablet mass and the applied force.

For example, an expression attributed to Heckel (17) has received considerable attention in recent years (10,14,18-21). In terms of porosity (E) it takes the form :-

$$\ln [E]^{-1} = KP + A \qquad \text{(Eq. 1)}$$

where P is the applied pressure; K is proportional to the reciprocal of the mean yield pressure; and A is a function of the initial porosity (i.e. when P = 0).

Hersey and Rees (18) used this equation to try to differentiate between compression by brittle fracture in the case of lactose and plastic deformation in the case of sodium chloride, but other workers (20,21) have reported the limitations of Heckel plots.

Reviews of compaction equations (22,23) suggest their number approximates to the number of workers in this field. However, many of the expressions have been shown to have applicability over only a limited range of applied force and for only a few materials. Certainly no universal relationship has yet emerged and is unlikely to do so.

In any case, this approach is concerned more with compression (reduction in volume) and only indirectly assesses the second major effect of compaction, namely consolidation (increase in mechanical strength). It can be argued that materials which readily form strong interparticulate bonds will lead to tablets of greater mechanical strength. However, because of these strong interactions, there will be a greater resistance to compression during the process than with poorly bonding materials. This will be translated into a greater energy requirement to make the stronger tablets.

This is one of the reasons why researchers attempted to measure the energy involved during the compaction of tablets (4,14,24). Energy transferred by the upper and lower punches is utilised for particle rearrangement, elastic-plastic deformation and/or brittle fracture and breaking of bonds in the material. The proportion of the total energy applied to the material which has been absorbed by it, can be estimated from the area under an appropriate force-displacement curve (25). An alternative to

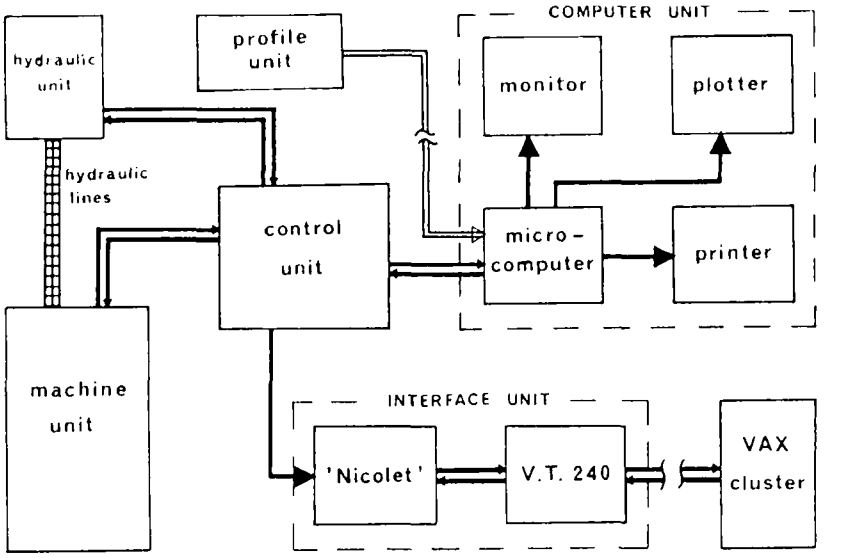

FIGURE 1
Units of a Compaction Simulator System (Schematic)

presenting energy consumption data is the power profile (i.e. energy per unit time) on which very little information exists in the literature (26,27).

THE COMPACTION SIMULATOR

As shown schematically in Figure 1, the "true" compaction simulator system used in the present work consists of the several units described below.

i. Hydraulic Unit :

The Hydraulic Pack (Mand Testing Machine Ltd. Stourbridge, U.K.) provides the power to move the tablet tooling, using hydraulic fluid under high pressure (up to 28MPa) at flow rates up to 170L/min for each actuator. An oil cooling heat exchanger utilizes chilled water (at a rate of 50L/min) to maintain the hydraulic fluid at a constant temperature (within 3°C).

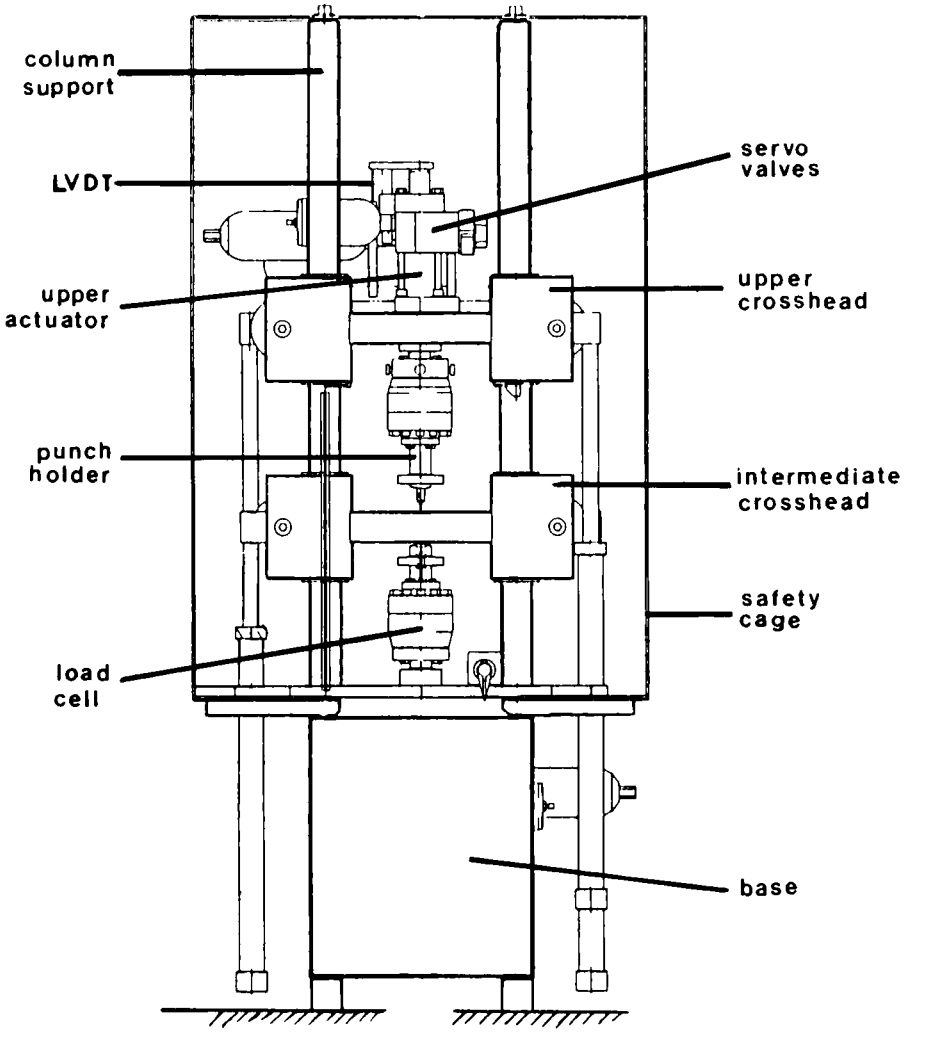

FIGURE 2
Components of the Machine Unit (Schematic)

Sophisticated filtration components in the hydraulic unit keep the hydraulic fluid free of particles which otherwise could seriously affect the servo valves and influence the actuator responses.

ii. Machine Unit :

The Machine Unit (Mand) is the actual press simulator and, as shown in Figure 2, comprises a 4 pillar servo hydraulic test machine with upper and

lower hydraulic actuators that are capable of applying forces up to 70kN. The upper crosshead incorporates the upper punch actuator, its servo valve assembly and the associated load and displacement transducers. The intermediate crosshead carries the versatile die table and small range displacement transducers. Both the upper and intermediate crossheads can be positioned vertically by means of hydraulic jacks. The lower punch actuator and its associated components are mounted on the base assembly. The two actuators accept interchangeable tool holders so that any standard (IPT) 'B', 'D' or 'F' punches can be used. Complementary interchangeable die holders can be securely clamped in the die table which forms part of the intermediate crosshead. Although the machine unit is large (58cm x 112cm x 241cm) and heavy (1235kg), precise vertical alignment of the tooling, at least as good as that of a new tablet press, is achieved.

The machine can generate forces in excess of 50kN at the face of punches moving at speeds up to 1.1m/sec. Therefore, for safety reasons, the entire area of the machine above the enclosed base is surrounded by a cage of armored clear plastic. A door in the front is used for access and is electronically interlocked with the control unit to prevent operation of the system with the door open.

iii. Control Console :

The Electronic Unit (Mand) is a 48cm rack mounting console into which several modules are fitted, as shown in Figure 3. These control the major parameters of load, position and strain associated with each punch. 'The Signal Read Out Modules' of the control unit include a 4 digit LED display providing a continuous or peak reading of either punch position, strain or load. This feature is particularly useful when setting up precise initial conditions for a test.

'Load Cell Amplifiers' provide complete conditioning at several ranges (10, 25, 50 and 100kN) for the upper and lower load cells. Signals from broad range, top and bottom punch position transducers that have two

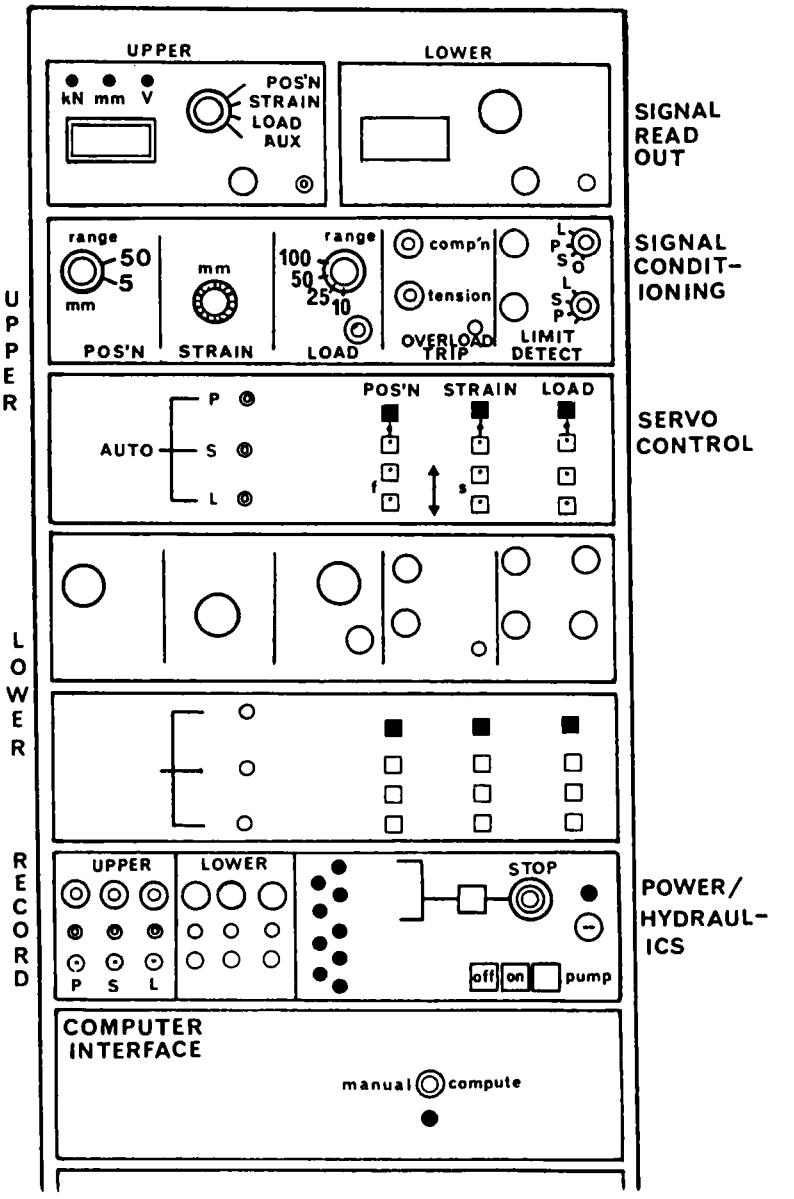

FIGURE 3
Components of the Control Unit (Schematic)

ranges (0 to 50mm and 0 to 5mm), are conditioned by 'Position Transducer Amplifiers'. Small movements of the upper and lower punches are monitored by narrow range strain transducers giving signals that are conditioned by 'Extensometer Amplifiers'. The 'Overload Modules' detect load signals beyond a preset range and warn the operator and/or initiate automatic unloading procedures, while 'Limit Detectors' function in a similar manner whenever readings of load or position fall outside a preset window.

The 'Servo Control Modules' enable the operator to run a machine cycle in either manual or automatic mode, based on position, strain or load information. The output signals from the electronic units associated with the force and displacement transducers can be retrieved by the operator via the 'External Recording Modules'.

The 'Power and Hydraulics Module' acts as a master on/off control center for the remote hydraulic system and also monitors the status of important operation parameters.

iv. Computer And Interface Unit :

Hardware :

The compaction simulator is controlled by an Apple][e microcomputer. The micro has a 128K extended RAM, a simulator interface card (M80-200) and is interfaced with an RGB color monitor, printer (Epson LX-80) and a plotter (Epson HI-80).

Since the Apple][e can only carry out a limited amount of data collection and storage, the system is interfaced to a main frame computer (a VAX 11/785 Cluster) via a digital storage oscilloscope (Nicolet # 4094). The latter has a capacity to capture 16K of data in 4 channels at rates ranging from 1 point every 200 secs up to 2 million points/sec. It therefore provides an accurate clock for timing compaction cycles.

Software :

In the present work, two major programs were used to operate the compaction simulator system. One of them was the "MAND Operating Programme" package which was written in BASIC with Machine Code subroutines for the microcomputer system, and consisted of several submenus including 'compaction test', 'waveform file processing', 'data analysis', 'mode selection' and 'interface check' options.

The second major program which was developed as a Master Data Base Program "COMSIM", was written in RPL (Research Programming Language) in conjunction with RSE (a scientific data management and analysis tool) for the main frame computer. The options available at COMSIM are as follows :-

1. "Waveform Menu" creates and stores theoretical compaction profiles of several tablet presses operating at different speeds as detailed later.
2. "Calibration Menu" stores the calibration data and applies a statistical regression analysis to them.
3. "Data Acquisition Menu" prompts the operator to set the parameters of the Mand Control Unit and Nicolet Oscilloscope correctly for a predetermined test condition. This menu also directs the user to follow the "MAND Operating Programme" and stores all information related to a compaction test.
4. "Data filing Menu" transfers data from the Nicolet Oscilloscope to the main frame computer and converts them into RSE tables.
5. "Data Processing Menu" applies the calibration factors (concerning the upper and lower punch forces and movements) and, when necessary, statistical analysis to the data given in RSE tables.
6. "Graphs Menu" creates plots for a number of techniques (such as Heckel, Force vs Displacement, Porosity vs Pressure, Force vs Time, Power vs Pressure plots etc.) and prints them out on a High Quality Laser Printer or on a plotter (Tektronix Model 4693D).

7. "Help Menu" functions as a trouble-shooting option.
8. Other auxilliary menus organize the directories for data storage and library purposes and serve for other parameters involved in data evaluation.

v. Profile Unit :

The ultimate aim of the simulator is to be able to mimic the precise compaction cycle of any tablet press in real time. To do this it is necessary to provide the system with co-ordinates of punch position with respect to time. The compaction profiles can usually be obtained from either theoretically known press geometry and conditions, or actual tooling position signals received from appropriate displacement transducers mounted on the press. Radio telemetry devices are commonly used to capture these actual compaction cycles of multi-station presses.

In the present work, theoretical compaction waveforms were obtained by using the following equation developed by Rippie and Danielson (28).

$$z = [\,(r_1 + r_2)^2 - (r_3 \sin wt - x)^2\,]^{1/2} \qquad \text{(Eq. 2)}$$

where z is the vertical displacement of the upper punch at time t ; r_1 and r_2 are the radii of the compression rolls and head O.D. respectively ; r_3 is the radial distance between the turret center and die cavity center (so called "pitch circle") ; x is the horizontal distance between the center of the upper punch and the center of vertical curvature of the punch head rim ; w is the turret angular velocity.

Using the above equation in conjunction with the master data base program (COMSIM), a library of compaction profiles was created for a number of tablet presses (including a Manesty Beta Press, "D" Press, Fette 3000) and provided for them to run at different speeds. These profiles were then transferred manually to the MAND Waveform File Diskette of the microcomputer and could be followed by the simulator during a compaction test.

Since the simulator is also capable of performing under load control, alternative profiles can be created from force readings (as a function of time). Such profiles may be of use in studying the strain changes under constant stress conditions, for example.

vi. Calibration of the System :

The load cells on the upper and lower actuators were calibrated using proving rings at the factory before delivery of the simulator. However the displacement transducers were not calibrated at the factory, therefore, an in situ calibration assembly consisting of a pair of digital micrometer calipers (Material Control Inc.) was rigidly mounted on the intermediate crosshead and firmly linked to the appropriate punch holders. These assemblies were used to perform calibration of the displacement transducers within $\pm$ 10μm accuracy and are routinely used to check calibrations.

Analog output signals from the load cells and displacement transducer conditioning units are digitised and converted to the physical units kN and mm respectively.

MATERIALS AND METHODS

A. MATERIALS :

To test the performance of the compaction simulator system, model powders known to exhibit varying degrees of compressibility and compactibility were selected. All the materials examined were used as received from the suppliers.

Avicel PH-101 (a microcrystalline cellulose, FMC Corporation) and Sodium Chloride Granular, USP (Mallinckrodt) were chosen as representative of plastically deforming materials. Materials that exhibit at least some brittle fracture were typified by Emcompress (Dibasic Calcium Phosphate, Dihydrate USP, Edward Mendell Co. Inc.), Lactose Fast Flo (Mc

Kesson and Robins), Sorbelite Fine Granular (a crystalline sorbitol NF, Edward Mendell Co. Inc.) and Sucrose, NF (Amstar Corporation). Phenacetin (Aldrich Chemical Co. Inc.) and Acetaminophen (Penco of Lyndhurst Inc.) were selected as elastically deforming materials.

B. METHODS :

As a preliminary, the true density of each material was first measured using a Helium Pycnometer (Micromeritics Autopycnometer #1320). This value was then multiplied by a constant pre-selected true volume (0.175mL for the work described here) to give the actual weight of material to be compacted.

A 10mm diameter flat-faced round tooling was installed. The punch faces were brought into contact and the system was loaded up to 35kN and the distortion of the punches was monitored. In order to measure the 'bedding in' effects of the punches into the punch holders, the above process was repeated with the upper and lower punches interchanged. The distortion of the lower punch alone is normally expected to be larger than that shown by the upper punch (shorter stem). However, when the 'bedding in' effect was considered it was observed that total distortion of the upper punch system (punch and holder) was larger than that of the lower system. It was also observed that when the punches were taken out and replaced, the distortion values differed significantly. Therefore the distortion factors were determined and the punches were not removed from their holders throughout this study. The values so obtained were 3.8μm/kN for upper punch and 3.3μm/kN for lower punch.

Initial compaction tests were then performed according to the following procedure :-

1. The profile of a 16 station rotary tablet press (type 'D' press), operating at 30rpm was selected for these experiments. However, much of

the published data on the materials to be studied has been generated on a single-station press. To facilitate comparison the initial tests described here, were carried out with a single-ended compression cycle.

2. Die wall and upper and lower punch faces were cleaned with methanol and then lubricated with a solution of magnesium stearate in acetone between each compaction cycle. An amount of material to produce 0.175mL true volume was poured into the die manually. Since the simulator was programmed to operate under 'Position' Control rather than 'Load' Control, it was necessary to make some initial tests for each material to determine the final tablet thickness at the corresponding applied pressure. The upper and lower punches were then positioned so as to produce a tablet at a maximum load of either 6.28kN (for experiments at 80MPa) or 31.42kN (for tests at 400MPa).

3. The compaction test was then initiated and upper and lower punch forces and movements were recorded at 0.2msec intervals throughout the test by the Nicolet Oscilloscope. The tablet was ejected manually and thickness, weight and crushing strength (Instron Model 1000) measurements were performed on the compact. In the latter test a constant platen velocity of 50mm/min was used, in conjunction with the peak reading feature. The data were converted to tensile strength units, using the method of Fell and Newton (29).

4. The experiment was repeated until five satisfactory replicates were achieved for a given material under specific test conditions. If the upper punch force fell outside 95-105% of the pre-determined value then the test was rejected. When a set of tests was completed, the data were transferred from the Nicolet Oscilloscope to the main frame computer and converted into RSE tables for manipulation by the methods to be described.

5. The experiments made under 400MPa pressure using the single-ended cycle at a press speed of 30rpm were then repeated to produce data at 150rpm, at 80MPa or from a double-ended pressing cycle.

TABLE 2. Properties of Tablets Made Under 400MPa at 30rpm *

Material	ρ_t	Within the Die			After Ejection		
		E_o	E_m	ΔE	E_e	w	S_T
Avicel PH 102	1.617	82	9.7	72.3	13.6	281	15.15
Sorbelite	1.538	61	8.0	53.0	9.1	269	7.74
Lactose	1.580	63	10.9	52.1	11.0	276	4.78
Emcompress	2.355	62	17.6	44.4	16.1	410	3.40
Sodium Chloride	2.156	41	6.8	34.2	6.5	376	1.72
Sucrose	1.585	68	7.8	60.2	10.1	275	0.26
Phenacetin	1.226	75	4.4	70.6	+	205	+
Acetaminophen	1.294	83	5.7	77.3	+	219	+

(*) : mean of five replicates ; ρ_t : true density, g/cm^3 ;
E_o : porosity (E%) when upper punch just touches the powder ;
E_m : E% at maximum pressure ; $\Delta E : E_o - E_m$;
E_e : E% after ejection ; w : weight, mg ;
S_T : tensile strength, MPa ; + : laminated / capped

RESULTS AND DISCUSSION

Application of pressure to a powder bed in a die results in a reduction in the volume of the powder bed, due to rearrangement and fracture of the particles and their elastic and plastic deformation (30). One of the methods used to try to determine the volume reduction mechanisms operating in a particular case, is the measurement of porosity changes during compaction. In the present work, since the forces on the upper and lower punches and their positions were simultaneously monitored during compaction of the powders, it was possible to measure the porosity of the compacts under

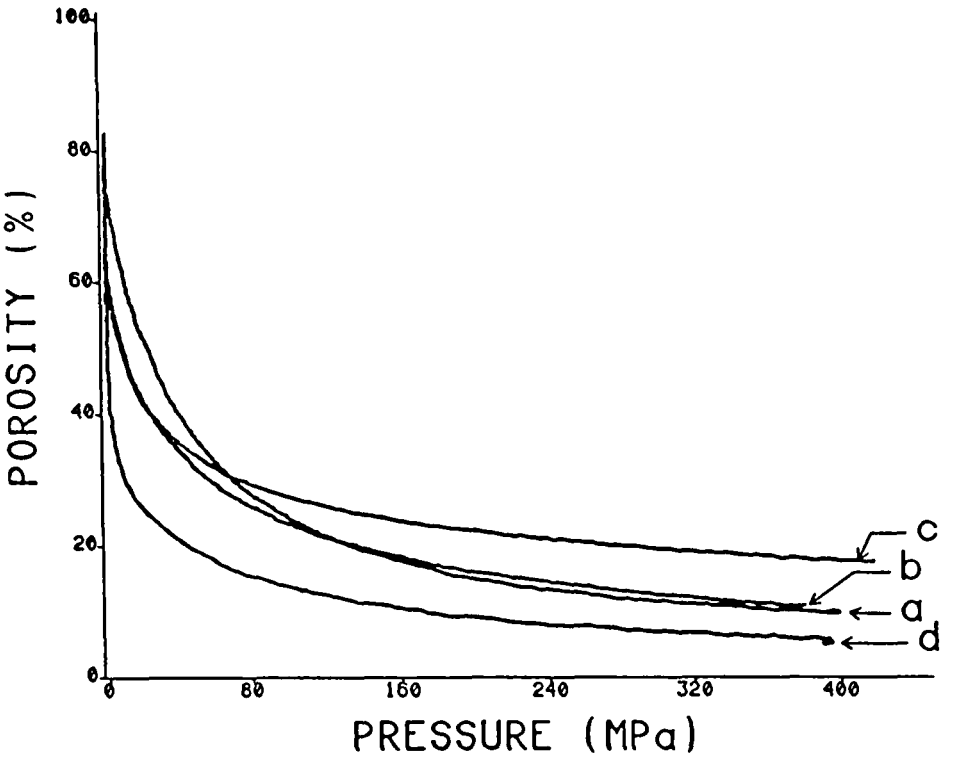

FIGURE 4a
Percentage Porosity vs Applied Pressure Profiles for Tablets Made Under 400MPa at 30rpm : (a) Avicel (b) Lactose (c) Emcompress (d) Acetaminophen

load. The following equation can be used for percentage porosity determination:-

$$E\ (\%) = 100 \cdot [1 - (V_t / V_c)] \qquad \text{(Eq. 3a)}$$

where V_t is the "true" volume of the material and V_c is the compact volume at a given pressure. Assuming that radial die-wall expansion during compaction is negligible, equation 3a may be written in the following form:-

$$E\ (\%) = 100 \cdot [1 - (H_t / H_c)] \qquad \text{(Eq. 3b)}$$

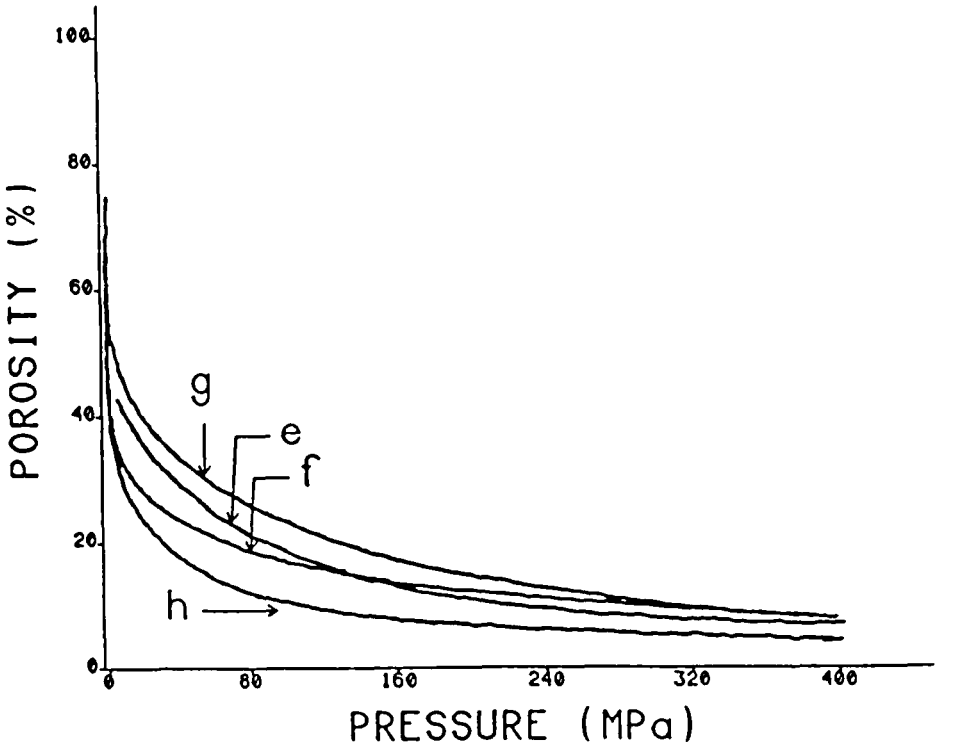

FIGURE 4b
Percentage Porosity vs Applied Pressure Profiles for Tablets Made Under 400MPa at 30rpm : (e) Sodium Chloride (f) Sucrose (g) Sorbelite (h) Phenacetin

where H_t is the theoretical "true" thickness of the compact at zero porosity and H_c is the compact thickness under some load (corrected for punch deformation). Table 2 includes percentage porosity data for the initial porosity (E_o), where the upper punch just touches the powder surface, minimum porosity (E_m) at maximum applied pressure and the porosity of the ejected tablet (E_e).

Initial porosity (E_o) values are markedly affected by the flow properties of the powder and by the method of filling material into the die cavity. Materials with poor flow properties may produce high E_o values as illustrated

in Figures 4a and 4b, in which percentage porosity data are plotted versus corresponding applied pressure. Phenacetin and Acetaminophen, which are poorly flowing powders, exhibited about 40% decrease in the porosity before any appreciable increase of pressure was detected. The E_e value of a tablet is normally expected to be higher than its E_m value, since the former includes possible elastic and viscoelastic expansion of the tablet occuring during decompression and after ejection. The results for some materials (Table 2) demonstrate the opposite effect, especially Emcompress, but the cause of this has not yet been identified.

No correlation was observed between the E_o and E_m values, nor between the total porosity change (ΔE) and say tensile strength values (See Table 2). The porosity versus pressure profiles derived from the data (Figure 4) are not predictive of the deformation characteristics of the powders nor the tensile strength of the actual tablets, but do confirm the higher resistance to compression of materials in which brittle fracture dominates (Emcompress).

Of the many relationships that have been proposed (22,23) to describe the changes in porosity (or tablet volume) due to increasing compressional force, the Heckel equation (Equation 1) seems to have received most recent attention (10,19,21). The reciprocal of the slope of the linear portion (i.e. 1/K) of Heckel Plots is generally defined as proportional to the mean yield pressure of a material and has been used to assess the dominant deformation mechanism. Some authors have pointed out that materials exhibiting fragmentation produce non-linear curves (18) and that the Heckel equation is strictly only applicable to plastically deforming materials (31,32).

The Heckel plots of the model materials used in this study (Figures 5a and 5b) were non-linear at pressures up to 400MPa. It was not therefore possible to postulate a yield pressure or a value for the constant 'A' in the Heckel equation. One possible explanation for our observations may simply

be that Heckel plots obtained under dynamic conditions are curved, but that regions where the change in slope is small, are present. If, unlike here (where there are up to 600 points on each curve), data are collected at only a few discrete points, then approximation to a straight line might be assumed. Certainly data collected under static conditions, where E values are calculated from 'out of die' measurements on tablets, would be expected to produce different results, since presumably elastic recovery of the tablet is contributing to its porosity under these conditions.

Attempts to fit other reported equations to the data led to the general conclusion that no one expression is likely to fit all materials over an appreciable range of applied force. For example the relationship proposed by Walker (33), given in Equation 4 :-

$$1 / (1 - E) = K_1 \log P + A_1 \qquad \text{(Eq. 4)}$$

where K_1 and A_1 are constants, was applied to our data.

One of the general characteristics of these plots (Figures 6a and 6b) was that they appeared to exhibit two inflection points dividing the curves into three zones. Middle regions of some of these plots (Figure 6b), which generally took place between 5-10MPa and 70-125MPa, produced high correlation coefficient (R) values on linear regression analysis. The data for the curves in Figures 6a and 6b are summarized in Table 3.

Walker (33) observed that K_1 values were greater for plastically deforming materials than those for brittle fractured ones, but no such correlation was evident in the present work. He also related the A_1/K_1 ratios to compressional behaviour and in Table 3, higher ratios were generally given by materials producing weaker tablets. Perhaps the most obvious factor is the anomalous behaviour of Avicel, a phenomenon reported by several other workers (10,24).

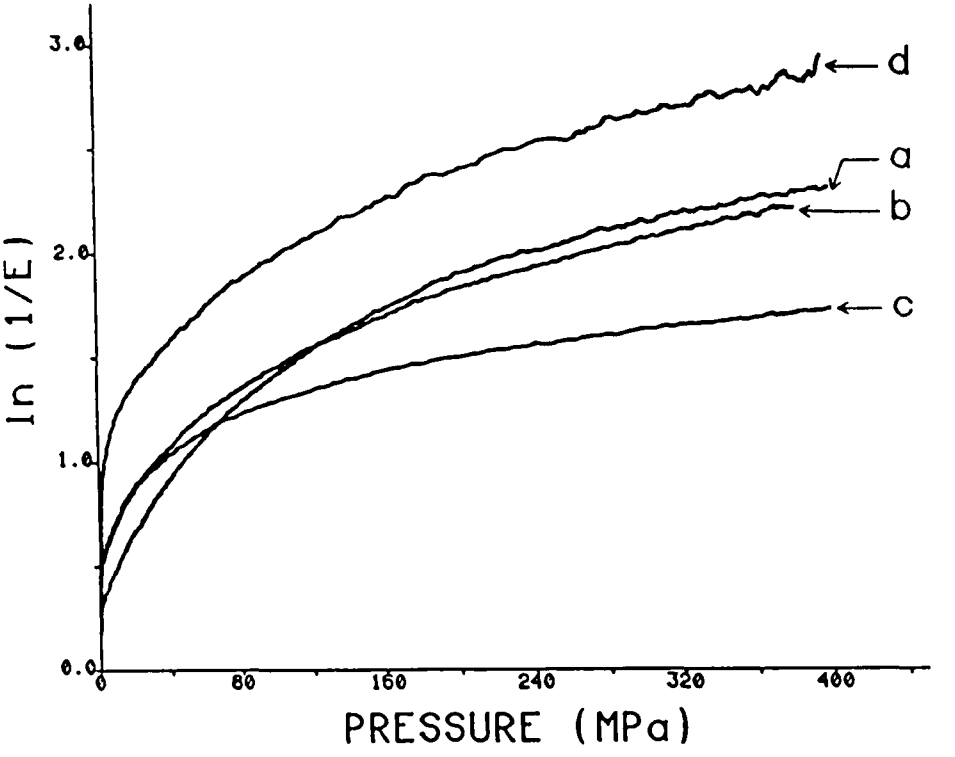

FIGURE 5a
Heckel Plots for Tablets Made Under 400MPa at 30rpm
(a) Avicel (b) Lactose (c) Emcompress (d) Acetaminophen

Fits to equations proposed by Shapiro (34) and Cooper and Eaton (35) were also attempted but compliance was poor.

Another common method assessing the compactional behaviour of materials is to use the plots of compressional force vs punch displacements (F-D curves) from which the work involved during tablet compaction can be calculated (24). Figure 7 shows a typical F-D curve obtained by plotting the upper punch force versus its displacement. However, when this technique was first applied in the present studies, the F-D curves exhibited unusual

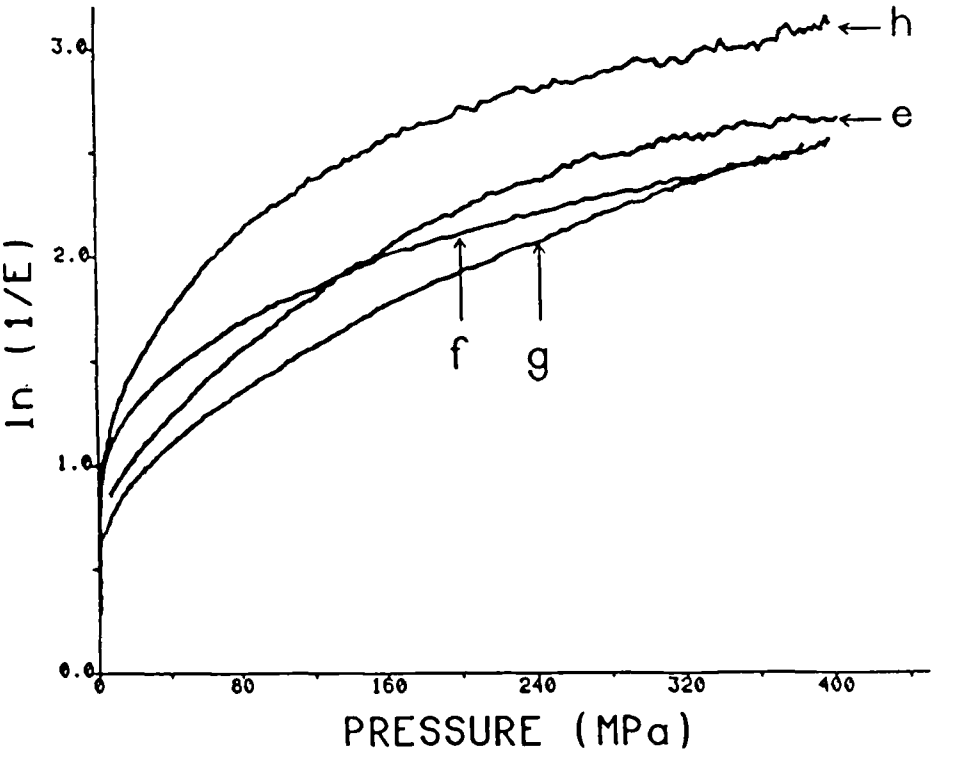

FIGURE 5b
Heckel Plots for Tablets Made Under 400MPa at 30rpm
(e) Sodium Chloride (f) Sucrose (g) Sorbelite (h) Phenacetin

shapes as shown in the same figure, i.e., demonstrated hysteresis. This difference can be explained by examining the forces and position of the upper and lower punches as a function of time (Figure 8). Although the lower punch was programmed to stay at a constant position, it moved very slightly downwards and then upwards during the compaction cycle. These small movements contributed to the force versus time profiles shown in the same figure. The explanation for this unusual behaviour is that in a single-station press the lower punch position is controlled mechanically, but in these studies, was achieved by hydraulic means. Similarly shaped F-D curves, showing hysteresis, are sometimes seen in data obtained from

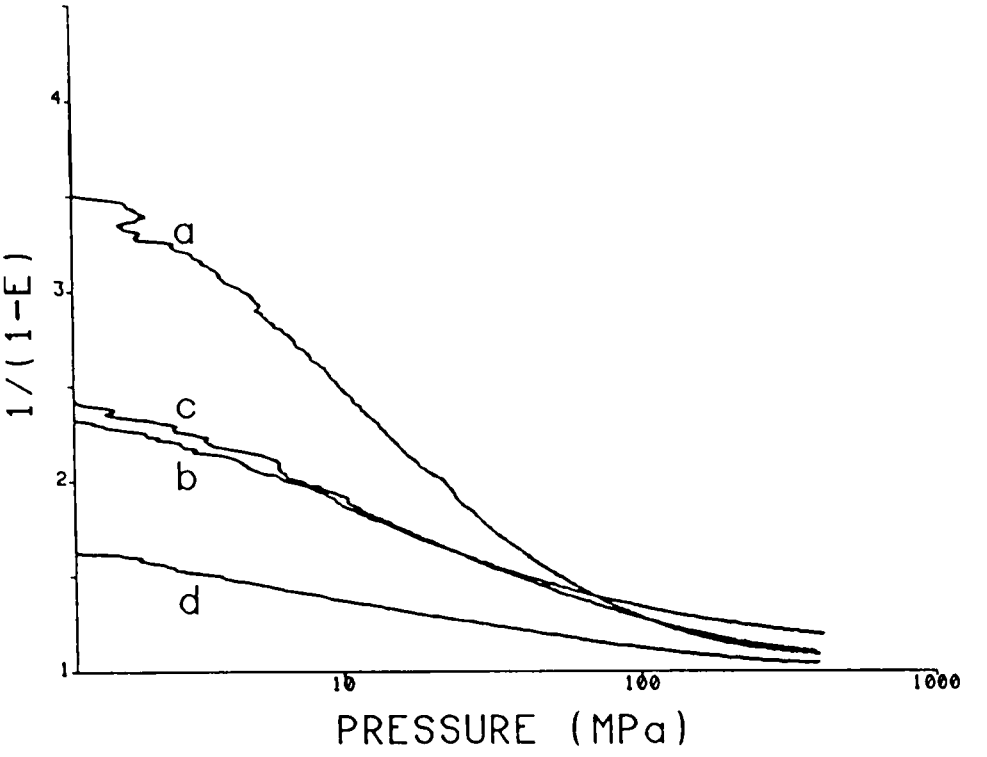

FIGURE 6a
Walker Plots for Tablets Made Under 400MPa at 30rpm
(a) Avicel (b) Lactose (c) Emcompress (d) Acetaminophen

rotary tablet machines (5), presumably because the lower punches are also free to make small movements against the overload mechanism.

Since these small movements of the lower punch may contribute significantly to the compression process, individual force and displacement data of both upper and lower punches were used to construct F-D curves. Figures 9a and 9b give examples of such curves obtained by plotting the arithmetic mean of the upper and lower punch forces versus powder bed height, i.e., the decrease in the distance between the upper and lower punches during the compaction event.

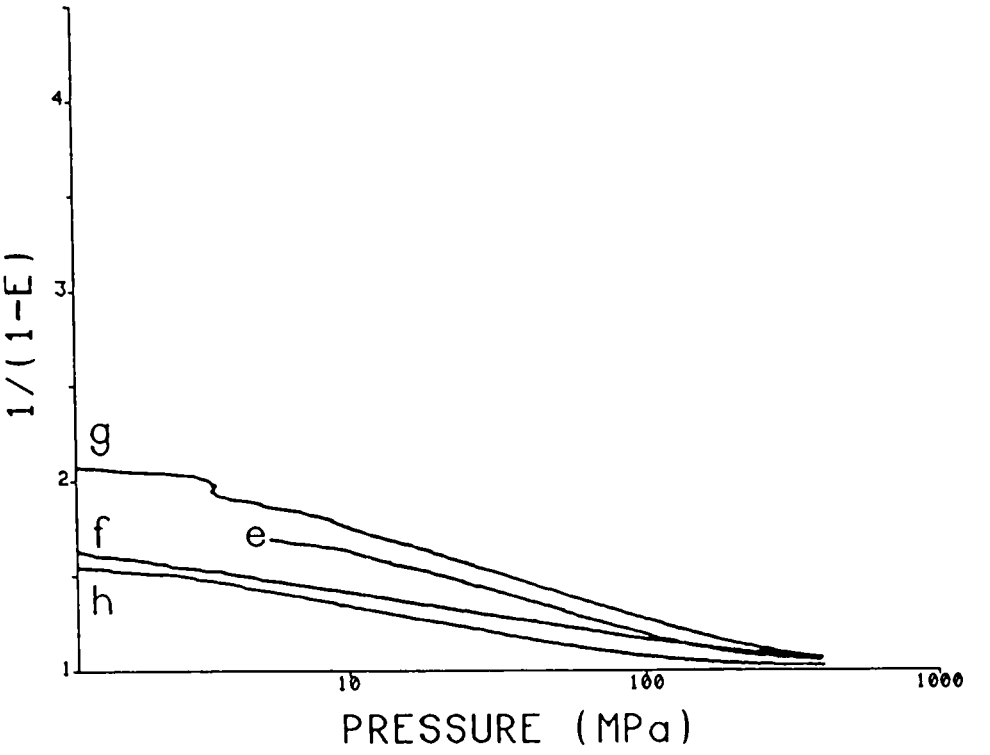

FIGURE 6b
Walker Plots for Tablets Made Under 400MPa at 30rpm
(e) Sodium Chloride (f) Sucrose (g) Sorbelite (h) Phenacetin

TABLE 3. Values* of the K_1, A_1 and A_1/K_1 Parameters from Equation 4

Material	K_1	A_1	A_1/K_1	R (data points)
Avicel PH 102	-1.285	3.720	2.895	0.9309 (154)
Lactose	-0.601	2.457	4.088	0.9992 (97)
Emcompress	-0.585	2.456	4.198	0.9879 (101)
Sorbelite	-0.487	2.245	4.610	0.9999 (81)
Sodium Chloride	-0.442	2.078	4.701	0.9995 (82)
Sucrose	-0.249	1.664	6.683	0.9998 (61)
Phenacetin	-0.251	1.622	6.462	0.9998 (61)
Acetaminophen	-0.275	1.613	5.866	0.9993 (68)

(*) : mean of five replicates (at 10-125MPa pressure range)

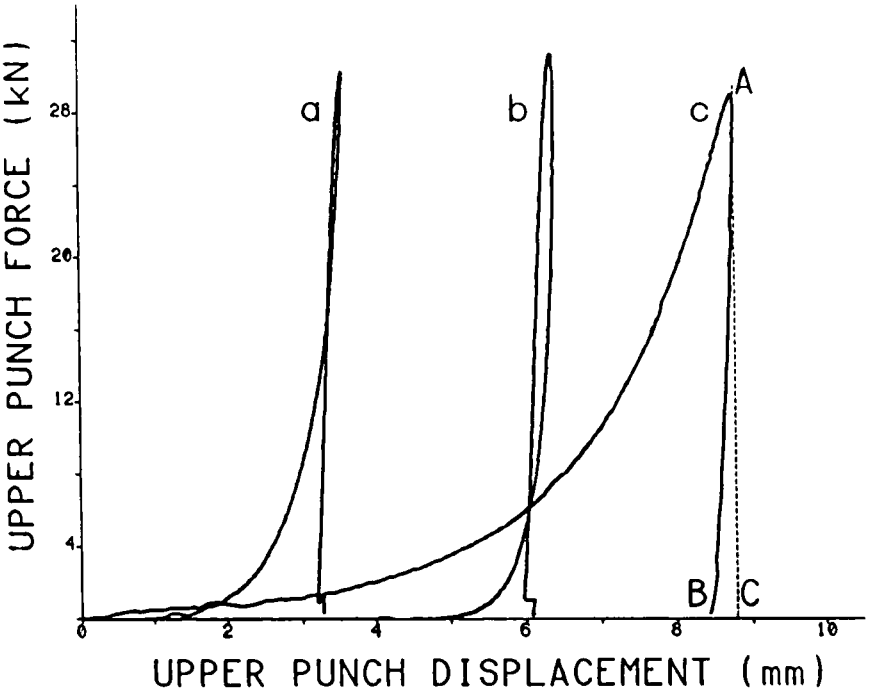

FIGURE 7
Typical F-D Profiles : (a) Sorbelite (b) Phenacetin (c) Theoretical
(The origin is where the upper punch just touches the powder)
Area Under OAC : Total Work of Compaction ;
Area Under BAC : Energy transferred back to the punch as a result of elastic recovery of the tablet

The area under F-D curves (OAB in Figure 7) has been used to estimate the energy consumption during the tabletting event. Krycer et al. (24) suggested that, since powders with different packing characteristics and different elastic and plastic deformational properties will absorb varying amounts of energy, it might be more useful to measure this "work of compaction", rather than other characteristics. Fell and Newton (36) formed the opinion that the work done on compaction of a powder mass is utilised both for volume reduction and particle bonding, and only the latter contributes to the strength of the tablet. The total work done on

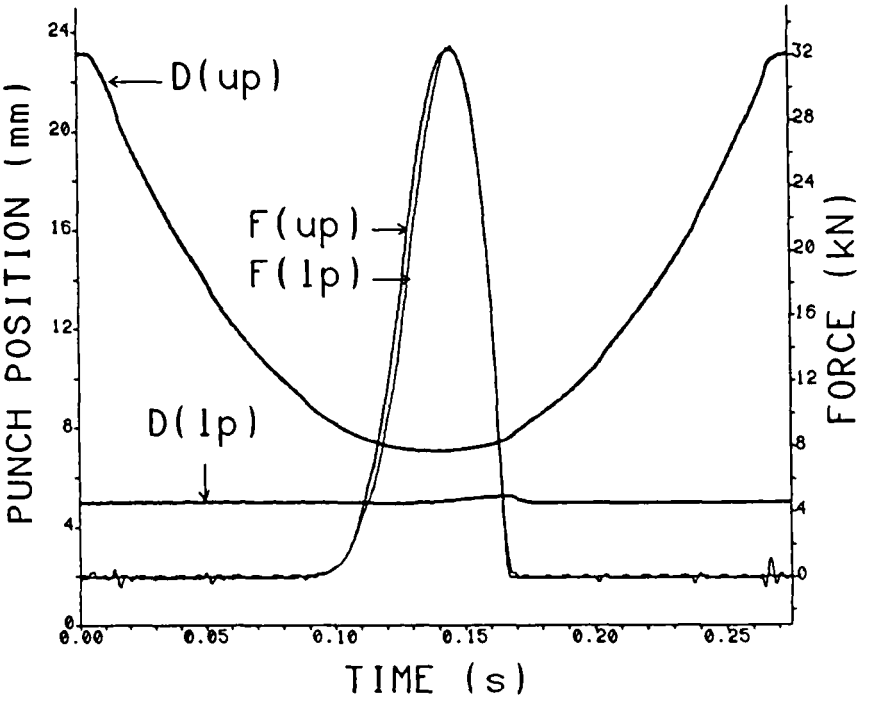

FIGURE 8
Punch Position vs Time and Applied Force vs Time Profiles for Acetaminophen Tablets Made Under 400MPa at 30rpm
D(up) and D(lp) are Upper and Lower Punch Positions respectively
F(up) and F(lp) are Upper and Lower Punch Forces respectively

compression is therefore not necessarily a criterion of tablet strength. This conclusion is not supported by the data reported here (see Table 4), where the rank order of total energy involved during compression and the tensile strength are similar. However, energy of compaction has not been defined consistently in the literature (24), therefore the rank order for the calculated work may be changed if the basis of calculation is changed (37). In our studies, total work of compaction (TWC) was calculated using the following equation, in which the contributions of the upper and lower punches to the total work were calculated separately:-

$$TWC = \left(\int_{X=0}^{Xmax(up)} F_{up}.dX_{up}\right) + \left(\int_{X=0}^{Xmax(lp)} F_{lp}.dX_{lp}\right) \qquad \text{(Eq. 5)}$$

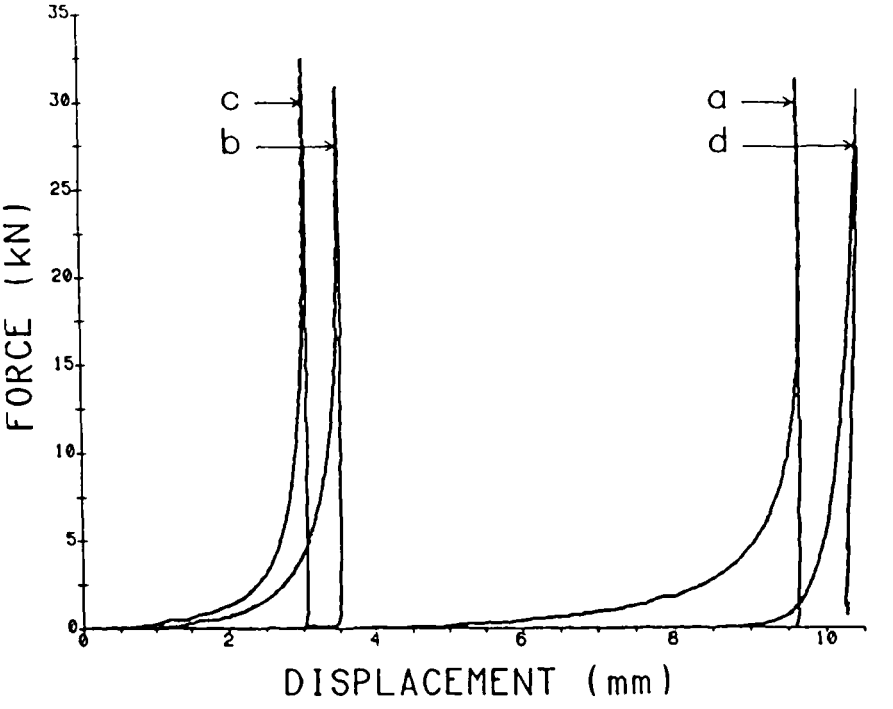

FIGURE 9a
F-D Profiles for Tablets Made Under 400MPa at 30rpm
(The origin is where the upper punch just touches the powder)
(a) Avicel (b) Lactose (c) Emcompress (d) Acetaminophen

where F_{up} and F_{lp} are the forces on the upper and lower punches respectively ; X_{up} and X_{lp} are the contributions of the upper and lower punches (respectively) to the decrease in the distance between them ; $X=0$ is the point where $E = E_o$ and maximum applied load was reached at $X_{max(up)}$ and $X_{max(lp)}$.

The data in Figures 10a and 10b (which gives total work versus corresponding pressure plots) and Table 4 seems to indicate that, as might be anticipated, stronger tablets are produced by materials where higher total work has been involved, There is some evidence that energy utilization for a

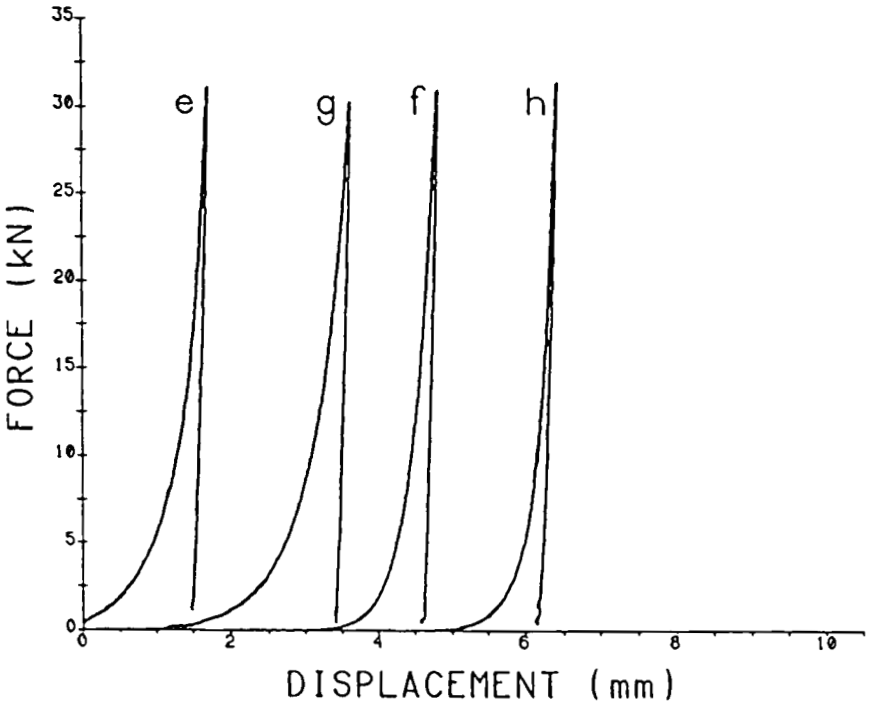

FIGURE 9b
F-D Profiles for the Tablets Made Under 400MPa at 30rpm
(The origin is where the upper punch just touches the powder)
(e) Sodium Chloride (f) Sucrose (g) Sorbelite (h) Phenacetin

plastically deformed material (such as Avicel) is generally higher than that for a brittle fractured (such as Emcompress) or an elastically deformed one (such as Phenacetin). However the data for Sodium Chloride known as a plastically deforming material did not support this conclusion and suggested that both plastic deformation and brittle fracture might be occuring. This view is in part agreement with the findings of Carstensen and Toure (38) who reported that Sodium Chloride exhibited dual behaviour.

In fact it may be unreasonable to expect that work of compaction plots can be used to distinguish the type of deformation of different materials,

TABLE 4. Properties of Tablets Made Under 400MPa at 30rpm*

Material	TWC (J)	APC (W)	ψ_n (W)	S_T (MPa)
Avicel PH 102	18.8	168	394	15.15
Sorbelite	15.2	225	471	7.74
Lactose	14.9	220	427	4.78
Emcompress	13.8	208	435	3.40
Sodium Chloride	12.1	250	360	1.72
Sucrose	10.1	130	382	0.26
Phenacetin	8.0	80	274	+
Acetaminophen	9.4	78	346	+

(*) : mean of five values (at maximum applied pressure) ;
TWC : total work of compaction ; APC : average power ;
ψ_n : instant power ; S_T : tensile strength of tablets ;
(+) : laminated and/or capped

since this concept does not contain a time variable in it, and so would not be sensitive to say plastic deformation with its time-dependent characteristics.

In addition, tablet presses run close to the set speed irrespective of the material being compacted. This means that if more work is required in a particular case, then it must be supplied at a greater rate.

For these reasons we have turned attention to the alternative way of presenting energy data using a power profile which does include the time

parameter. Power data for a small fraction of the total tabletting cycle time (ψ_n) can be calculated from :

$$\psi_n = (\Delta d_n / t_n) \cdot [(\Delta F_n / 2) + F_n] \qquad \text{(Eq. 6)}$$

where Δd_n is the distance the punch moves and ΔF_n is the change in the applied force during the interval t_n. F_n is the force at the beginning of t_n.

Plots of ψ_n against applied pressure (P) have the characteristic shape shown in Figures 11a and 11b, with ψ_n values going through a maximum. This is to be anticipated since power is zero initially and again at the point of maximum compression (no downward punch movement at this instant). The maximum corresponds to the point of inflexion on the force versus time profile as shown by the data for Avicel for example (Figure 11c), but no rank order correlation of ψ_n with either type of deformation, or tablet tensile strength, is seen.

A more discriminating pattern emerges if the average power consumption (APC) is calculated from the following equation :

$$\text{APC (Watt)} = \left(\int_{X=0}^{Xmax} F.dX\right) / t \qquad \text{(Eq. 7)}$$

where F is the applied force ; X is the decrease in the distance between the upper and lower punches ; $X=0$ and X_{max} are the points where $E=E_o$ and $E=E_m$ respectively ; t is the time for which the powder has been compressed.

Figures 12a and 12b give the power profiles obtained by plotting this average power consumption versus corresponding applied pressure. A common feature of these profiles is that although all materials demonstrated a continuously decreasing rate of energy utilization as the pressure was increased, the slopes of the plots could be clearly divided into two groups, corresponding to those where strong or weak tablets were produced.

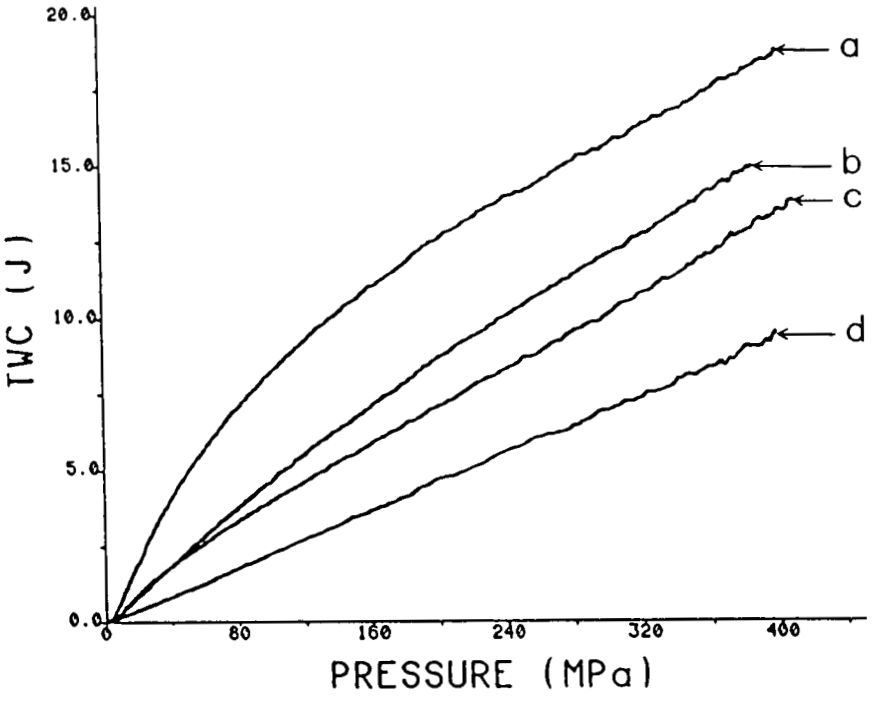

FIGURE 10a
Total Work of Compaction vs Applied Pressure Profiles
for Tablets Made Under 400MPa at 30rpm
(a) Avicel (b) Lactose (c) Emcompress (d) Acetaminophen

The method used to determine the time interval variable and to present power data can significantly change both the magnitude and rank order of power consumption. Armstrong and Palfrey (27) applying three different power equations to the same data, obtained different total power expenditures. Therefore the definition of the time variable and the way of calculating power must be carefully chosen if power expenditure is to be correlated with the compactional characteristics of a powder. It is acknowledged that a much more detailed investigation will be necessary before the tentative suggestions reported here can be stated with certainty.

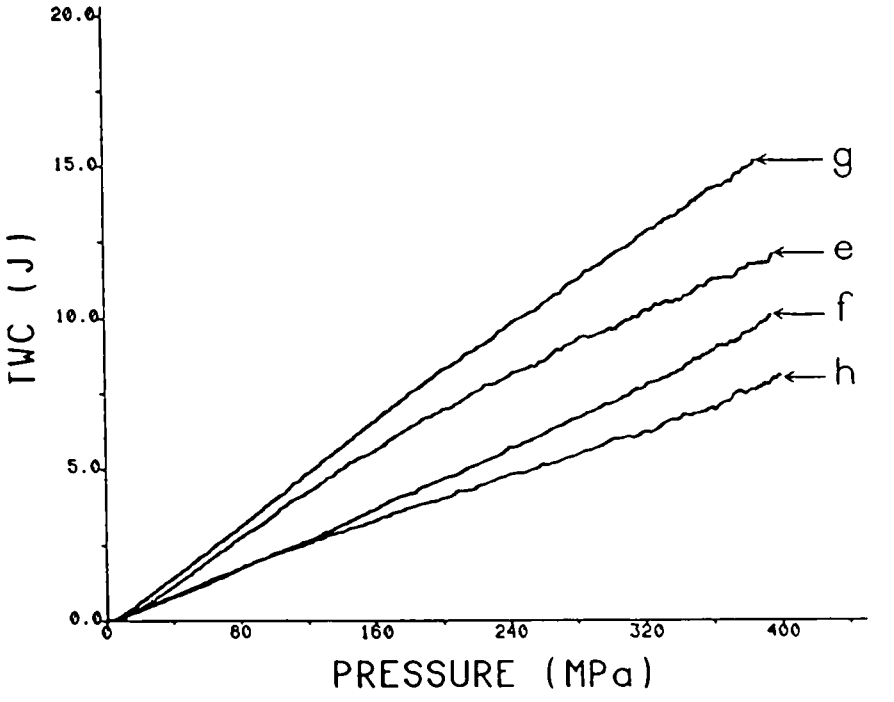

FIGURE 10b
Total Work of Compaction vs Applied Pressure Profiles
for Tablets Made Under 400MPa at 30rpm
(e) Sodium Chloride (f) Sucrose (g) Sorbelite (h) Phenacetin

The time frame of tabletting events discussed so far (press speed of 30rpm) is close to the maximum of the slower rotary tablet machines. To test the effect of higher speed tabletting, certain experiments were repeated at a rate of 150rpm. The data obtained are summarized in Figures 13a and 13b and indicate general rank order agreement with curves obtained at the slower speed, except for the region below say 30MPa applied pressure. The major reason for the unusual response at low loading was a lack of sufficient reference points on the waveform to permit the system to generate a smooth profile. The number of points is currently limited by the time needed by the

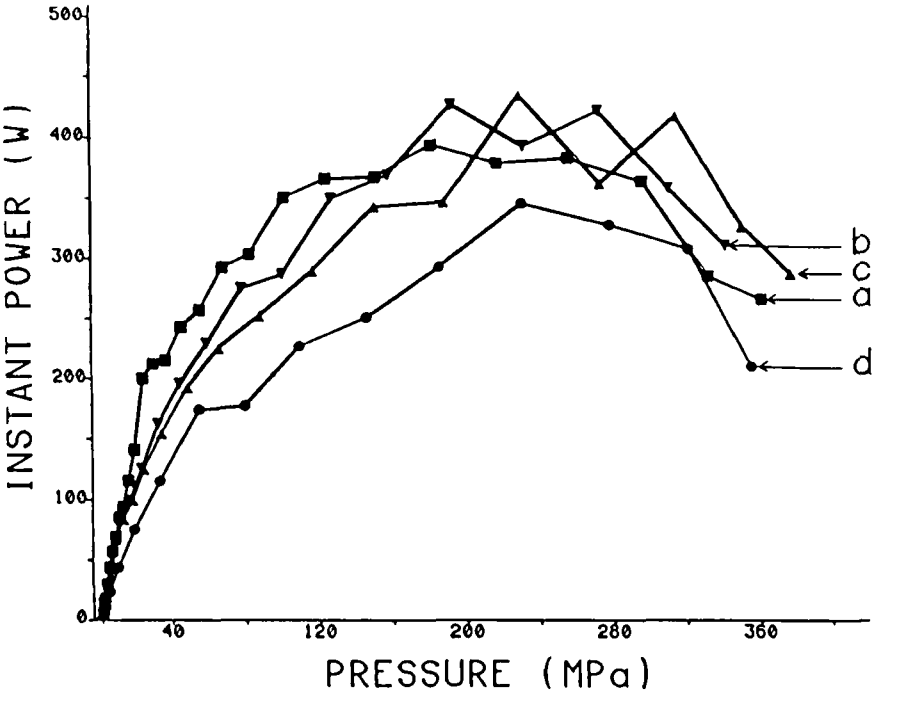

FIGURE 11a
Instant Power vs Applied Pressure Profiles for Tablets
Made Under 400MPa at 30rpm (time interval (t_n) is 3.2msec)
(a) Avicel (b) Lactose (c) Emcompress (d) Acetaminophen

microprocessor to calculate and issue instructions to the servo-mechanisms. Modifications to improve this performance are being developed. In addition the seismic effect resulting from rapid changes in velocity of the mass in front of the load cells (punch holder plus punch itself), especially at the beginning and end of a cycle is more pronounced at higher operating speeds (See Figures 14a and 14b). This effect could be minimised by the use of smaller tooling and lighter holders, made out of aluminum for example.

The maximum compressional pressure of 400MPa is higher than normally used for commercial tablets. In order to observe behaviour at the

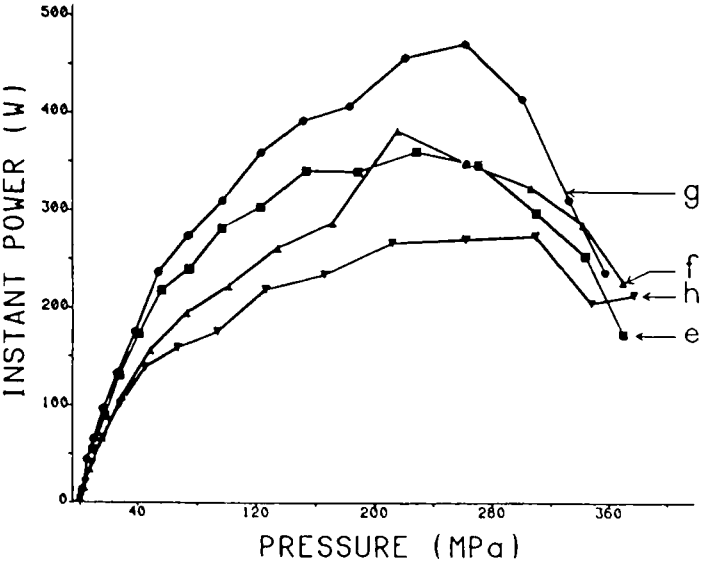

FIGURE 11b
Instant Power vs Applied Pressure Profiles for Tablets Made Under 400MPa at 30rpm (time interval (t_n) is 3.2msec) (e) Sodium Chloride (f) Sucrose (g) Sorbelite (h) Phenacetin

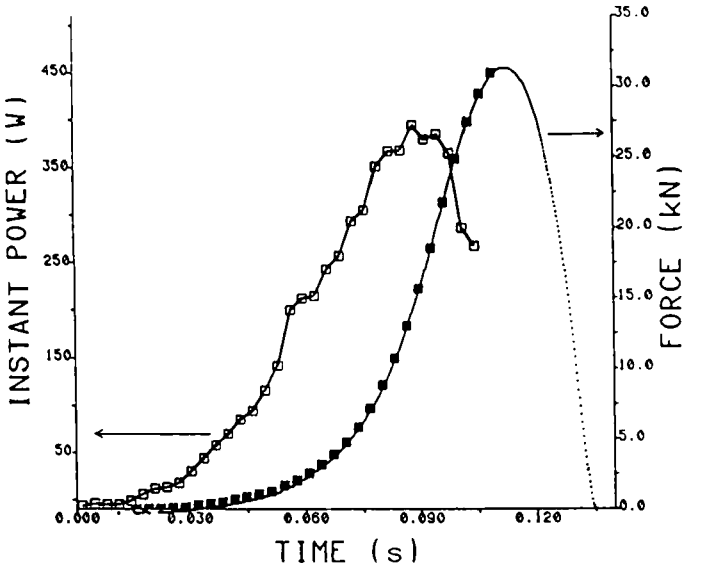

FIGURE 11c
Instant Power vs Time and Applied Force vs Time Profiles for Avicel Tablets Made Under 400MPa at 30rpm (time interval (t_n) is 3.2msec)

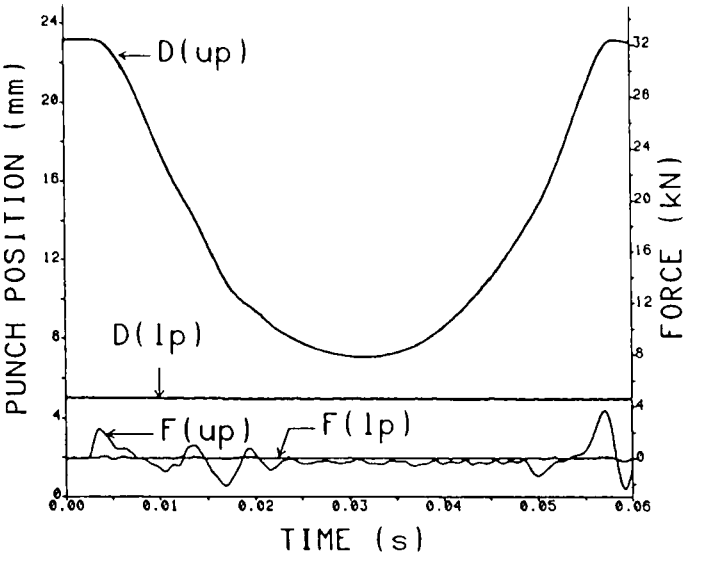

FIGURE 14a
Punch Position vs Time and Applied Force vs Time Profiles
for a Blank Run (No Powder in the Die) at 150rpm
D(up) and D(lp) are Upper and Lower Punch Positions respectively
F(up) and F(lp) are Upper and Lower Punch Forces respectively

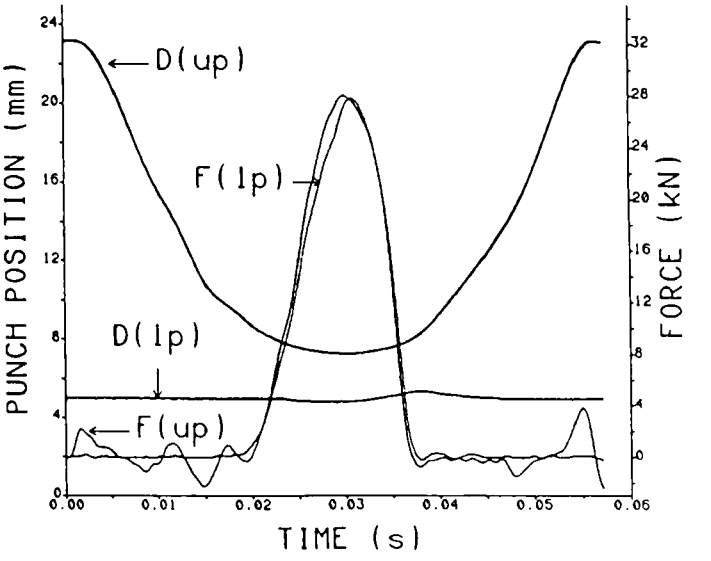

FIGURE 14b
Punch Position vs Time and Applied Force vs Time Profiles for
Acetaminophen Tablets Made Under 400MPa at 150rpm
D(up) and D(lp) are Upper and Lower Punch Positions respectively
F(up) and F(lp) are Upper and Lower Punch Forces respectively

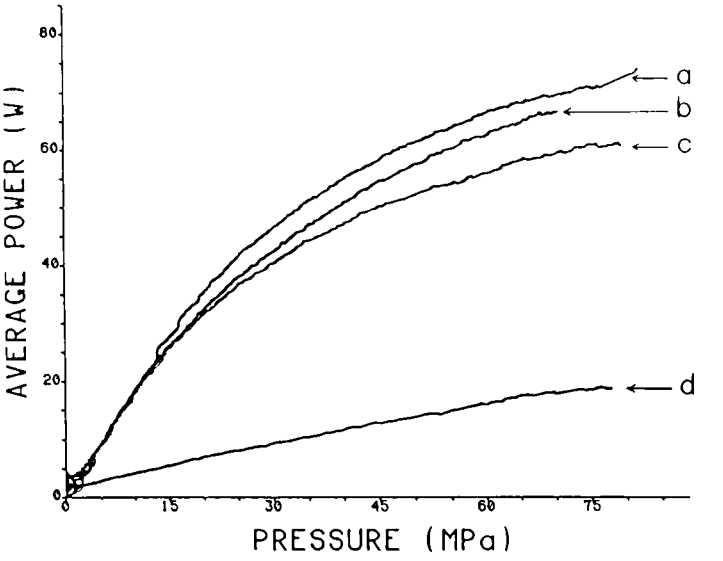

FIGURE 15a
Average Power Consumption vs Applied Pressure Profiles for Tablets Made Under 80MPa at 30rpm
(a) Avicel (b) Lactose (c) Emcompress (d) Acetaminophen

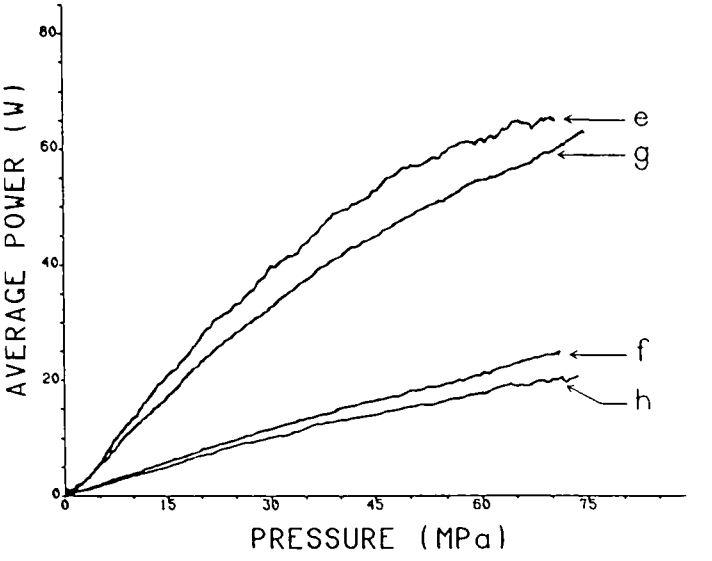

FIGURE 15b
Average Power Consumption vs Applied Pressure Profiles for Tablets Made Under 80MPa at 30rpm
(e) Sodium Chloride (f) Sucrose (g) Sorbelite (h) Phenacetin

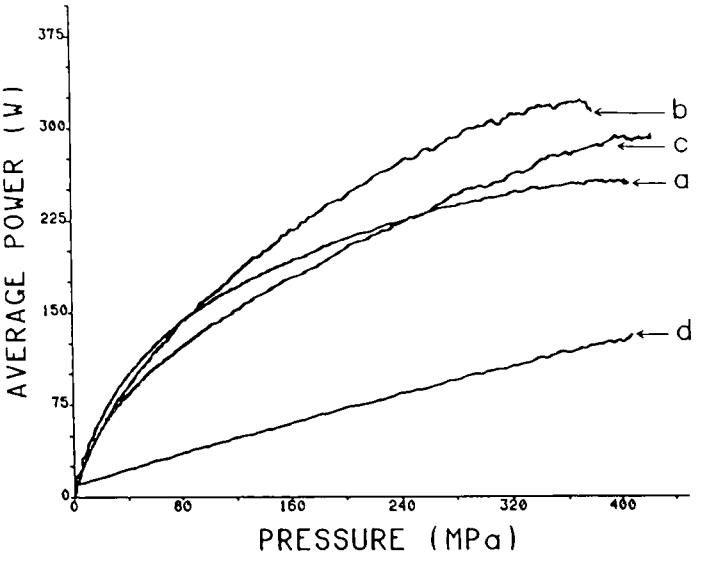

FIGURE 16a
Average Power Consumption vs Applied Pressure Profiles for Tablets Made Under 400MPa at 30rpm (Double-Ended Profile) (a) Avicel (b) Lactose (c) Emcompress (d) Acetaminophen

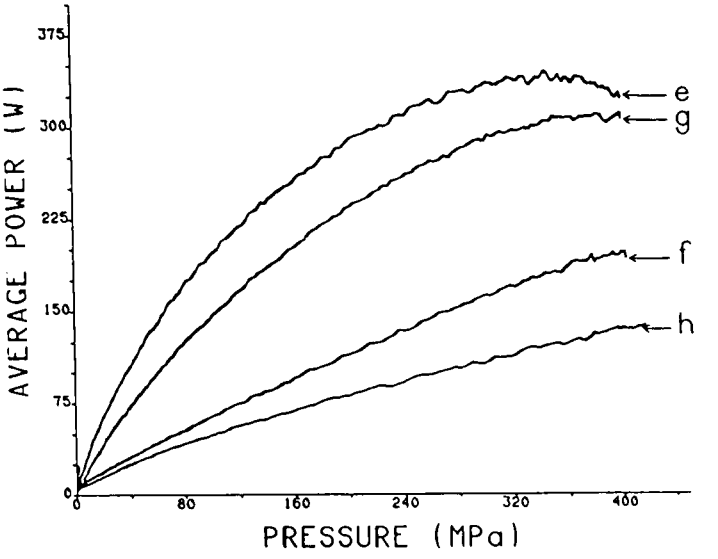

FIGURE 16b
Average Power Consumption vs Applied Pressure Profiles for Tablets Made Under 400MPa at 30rpm (Double-Ended Profile) (e) Sodium Chloride (f) Sucrose (g) Sorbelite (h) Phenacetin

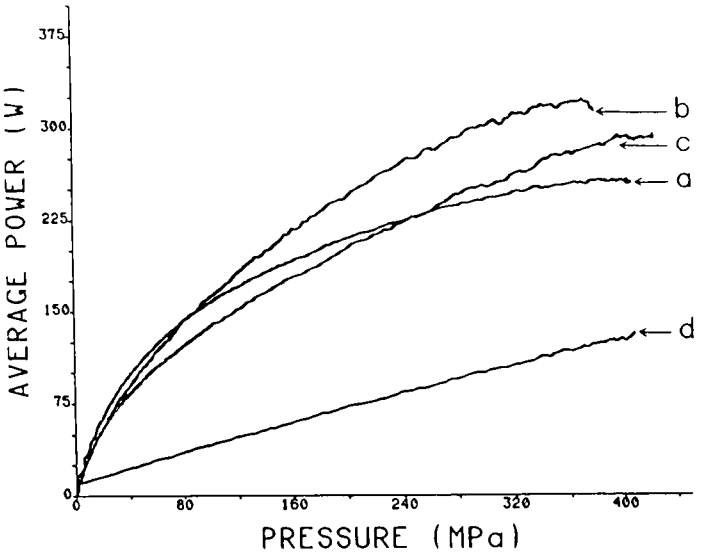

FIGURE 16a
Average Power Consumption vs Applied Pressure Profiles for Tablets Made Under 400MPa at 30rpm (Double-Ended Profile) (a) Avicel (b) Lactose (c) Emcompress (d) Acetaminophen

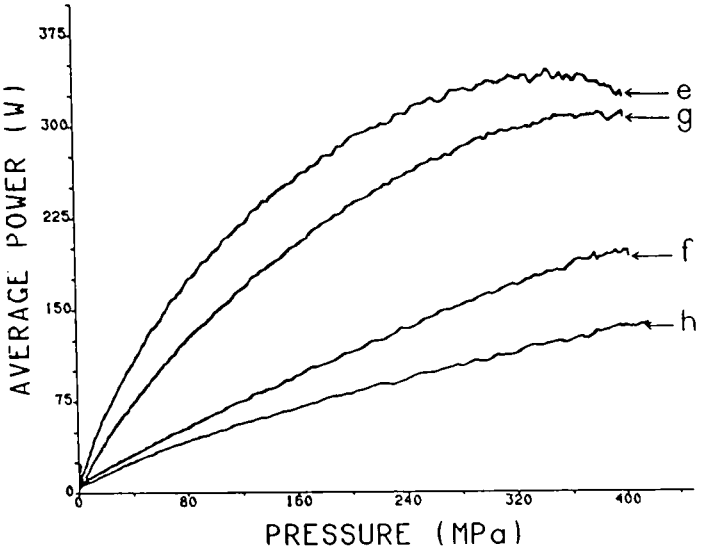

FIGURE 16b
Average Power Consumption vs Applied Pressure Profiles for Tablets Made Under 400MPa at 30rpm (Double-Ended Profile) (e) Sodium Chloride (f) Sucrose (g) Sorbelite (h) Phenacetin

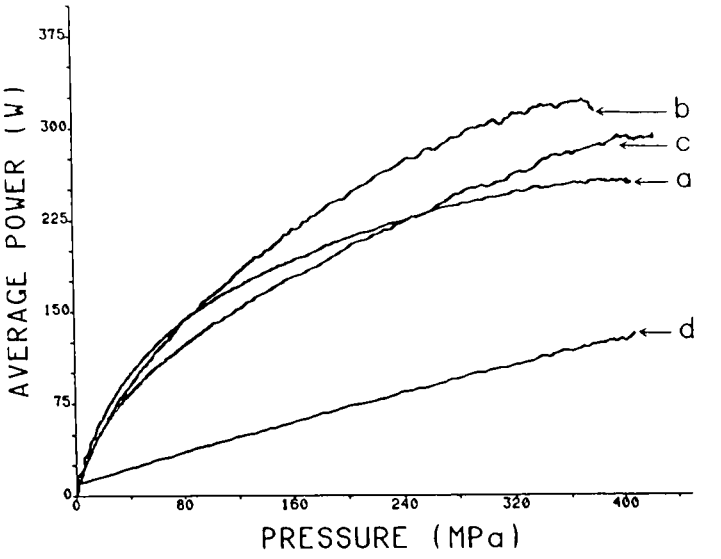

FIGURE 16a
Average Power Consumption vs Applied Pressure Profiles for Tablets Made Under 400MPa at 30rpm (Double-Ended Profile) (a) Avicel (b) Lactose (c) Emcompress (d) Acetaminophen

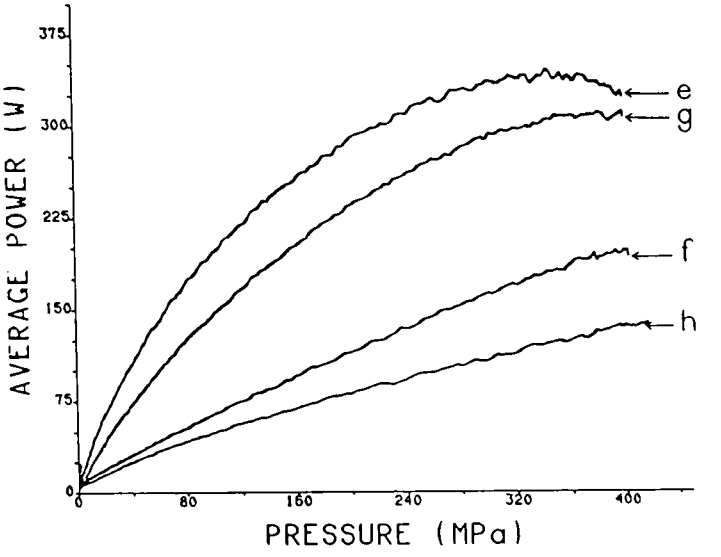

FIGURE 16b
Average Power Consumption vs Applied Pressure Profiles for Tablets Made Under 400MPa at 30rpm (Double-Ended Profile) (e) Sodium Chloride (f) Sucrose (g) Sorbelite (h) Phenacetin

TABLE 5. Comparison of APC and S_T values of tablets made under different tablet conditions *

Material	SINGLE-ENDED PRESSING						DOUBLE-ENDED	
	400MPa 30rpm		400MPa 150rpm		80MPa 30rpm		400MPa 30rpm	
	APC	S_T	APC	S_T	APC	S_T	APC	S_T
Avicel PH 102	168	15.15	1024	13.52	74	5.73	253	14.98
Sorbelite	225	7.74	1217	9.47	63	2.14	315	8.34
Lactose	220	4.78	1339	7.31	61	0.91	313	6.24
Emcompress	208	3.40	1135	2.72	59	0.78	291	2.82
Sodium Chloride	250	1.72	1438	1.78	65	0.55	325	1.83
Sucrose	130	0.26	836	+	24	+	189	+
Phenacetin	80	+	665	+	21	+	134	+
Acetaminophen	78	+	645	+	19	+	123	+

(*) : mean of five values (at maximum applied pressure) ;
APC : average power, W ; S_T : tensile strength of tablets, MPa ;
(+) : laminated and/or capped

lower end of this range in more detail, certain of the experiments were repeated at a maximum pressure of 80MPa. The power plots obtained under these conditions are illustrated in Figures 15a and 15b. As seen with the high load data, these curves enabled materials which did not produce strong tablets to be distinguished from those that did. The latter resulted in plots with greater curvature and significantly higher initial slopes. A comparison of the APC values and tensile strengths of the tablets is also given in Table 5 and the same rank order correlation as with the 400MPa data is seen.

It has been argued that data obtained on slow single station tablet presses is of limited value in predicting likely performance in a high speed multi-station machine. As a final exercise in these preliminary tests with the simulator, the compaction profile was changed to double-ended pressing in order to mimic the action of a rotary press.

Comparative data obtained by single and double ended pressing cycles are shown in Figures 16a and 16b. These plots seem to indicate that double-ended pressing of itself has little effect on the APC profiles produced by the simpler single-ended cycle. Lactose is the only material where double-ended action resulted in a significant increase ($\sim$ 30%) in the tensile strength of the tablets (See Table 5). Conversely the Emcompress tablets were somewhat weaker.

CONCLUSIONS

The work described in this introductory paper demonstrates the utility of the compaction simulator and introduces some types of data which can be easily generated. The possibilities are far from exhausted and additional modes of operation, such as measurements under constant stress or constant strain, are being tested. In addition, system modifications to facilitate well controlled high speed experiments and the significance of time as a variable are in progress.

However, these initial experiments do confirm the non-linearity of Heckel plots as reported by other workers and the lack of universal applicability in some other compaction equations. The potential usefulness of total work and 'power' plots is also demonstrated and is being more fully investigated, as are the variables of formulation, compaction cycle and tooling geometry on these parameters. It is interesting to note that double-ended pressing (as opposed to single-ended pressing) did not significantly alter the power profiles. It follows that it may therefore be possible to obtain relevant data from single-station presses, providing compaction time is not a critical parameter.

ACKNOWLEDGEMENT

The authors wish to thank Smith Kline & French Laboratories for sponsoring a post doctoral appointment to one of us (MÇ).

REFERENCES

1. T. Higuchi, E. Nelson and L. W. Busse, J. Am. Pharm. Ass., Sci. Ed., 43, 344 (1954).
2. E. Shotton, J. J. Deer and D. Ganderton, J.Pharm. Pharmacol., 15, 106T (1963).
3. F. W. Goodhart, G. Mayorga, M. N. Mills and F. C. Ninger, J. Pharm. Sci., 57, 1970 (1968).
4. C. J. de Blaey and J. Polderman, Pharm. Weekblad., 106, 57 (1971).
5. J. T. Walter and L. Augsburger, Pharm. Technol., 10(2), 26 (1986).
6. E. T. Cole, J. E. Rees and J. A. Hersey, J.Pharm. Pharmacol., 23, suppl. 258S (1971).
7. M. Çelik and D. N. Travers, Drug Dev. & Ind. Pharm. 11, 299 (1985).
8. B. M. Hunter, D. G. Fisher, R. M. Pratt and R. C. Rowe, J. Pharm. Pharmacol., 28, 65P (1976).
9. S. C. Mann, D. B. Bowen, B. M. Hunter, R. J. Roberts, R. C. Rowe and R. H. T. Tracy, J. Pharm. Pharmacol., 33, suppl. 25P (1981).
10. R. J. Roberts, and R. C. Rowe, J. Pharm. Pharmacol., 37, 377 (1985).
11. K. G. Pitt, J. M. Newton, R. Richardson and P. Stanley, J. Pharm. Pharmacol., 39, suppl. 65P (1987).
12. S. D. Bateman, M. H. Rubinstein and P. Wright, J. Pharm. Pharmacol., 39, suppl. 66P (1987).
13. R.F. Lammens, T.B. Liem, J. Polderman and C.J. de Blaey, Powder Technol., 26, 169 (1980).
14. G. Ragnarsson and J. Sjogren, J. Pharm. Pharmacol, 37, 145 (1985).
15. C. Carstensen, J. Marty, F. Puisieux and H. Fessi, J. Pharm. Sci., 70, 222 (1981).

16. D. N. Travers and M. P. H. Merriman, J. Pharm. Pharmacol., 22, suppl. 17S (1970).
17. R. W. Heckel, Trans. Metall. Soc. AIME, 221, 671 (1961).
18. J. A. Hersey and J. E. Rees, Proceedings of the 2nd Particle Size Analysis Conf., Society for Analytical Chemistry, Bradford, 33 (1970).
19. P. York and N. Pilpel, J. Pharm. Pharmacol., 25, suppl. 1P (1973).
20. P. J. Rue and J. E. Rees, J. Pharm. Pharmacol., 30, 642 (1978).
21. M. Duberg and C. Nystrom, Powder Technol., 46, 67 (1986).
22. K. Kawakita and K. H. Ludde, Powder Technol., 4, 61 (1970/71).
23. G. Bockstiegel, Proceedings of the 2nd Int. Conf. on the Compaction and Consolidation of Particulate Matter, Brighton (1975).
24. I. Krycer, D. G. Pope and J. A. Hersey, Int. J. Pharmaceutics, 12, 113 (1982).
25. T. M. Jones, Acta Pharm. Tech. 6, 141 (1978).
26. N. A. Armstrong, N. M. A. H. Abourida and A. M. Gough, J. Pharm. Pharmacol., 35, 320 (1983).
27. N. A. Armstrong and L. P. Palfrey, J. Pharm. Pharmacol., 39, 497 (1987).
28. E. G. Rippie and D. W. Danielson, J. Pharm. Sci., 70, 476 (1981).
29. J. T. Fell and J. M. Newton, J. Pharm. Pharmacol., 20, 657 (1968).
30. J. M. Newton and D. J. W. Grant, Powder Technol., 9, 295 (1974).
31. J.A. Hersey, E. T. Cole and J. E. Rees, Proceedings of the 1st Int. Conf. on the Compaction and Consolidation of Particulate Matter, Brighton, 165 (1973).
32. A. H. De Boer, G. K. Bolhuis and C. F. Lerk, Powder Technol., 20, 75 (1978).
33. E. E. Walker, Trans. Faraday Soc., 19, 73 (1923).
34. I. Shapiro, Ph.D. Thesis, University of Minnesota (1944).
35. A. R. Cooper and L. E. Eaton, J. Am. Ceram. Soc., 45, 97 (1962).
36. J. T. Fell and J. M. Newton, J. Pharm. Sci., 60, 1428 (1971).
37. M. Çelik, Ph.D. Thesis (CNAA), Leicester Polytechnic (1984).
38. J. T. Carstensen and P. Toure, Powder Technol., 26, 199 (1980).